

TO THE EDITOR:

Myb drives B-cell neoplasms and myeloid malignancies in vivo

Tim Pieters,^{1-3,*} André Almeida,^{1-3,*} Sara T'Sas,¹⁻³ Kelly Lemeire,^{4,5} Tino Hochepped,^{4,5} Geert Berx,³⁻⁵ Alex Kentsis,⁶⁻⁸ Steven Goossens,^{1-3,9,*} and Pieter Van Vlierberghé^{1-3,*}

¹Department of Biomolecular Medicine, and ²Center for Medical Genetics, Ghent University and University Hospital, Ghent, Belgium; ³Cancer Research Institute Ghent (CRIG), Ghent, Belgium; ⁴Department of Biomedical Molecular Biology, and ⁵Center for Inflammation Research, VIB, Ghent, Belgium; ⁶Molecular Pharmacology Program, Sloan Kettering Institute, New York, NY; ⁷Departments of Pediatrics, Pharmacology, and Physiology & Biophysics, Weill Cornell Medical College, Cornell University, New York, NY; ⁸Tow Center for Developmental Oncology, Department of Pediatrics, Memorial Sloan-Kettering Cancer Center, New York, NY; and ⁹Department of Diagnostic Sciences, Ghent University, Ghent, Belgium

The proto-oncogene *MYB* encodes the transcription factor c-MYB (cellular MYB, hereafter called MYB), which is often upregulated or aberrantly activated in cancer, including hematological malignancies.^{1,2} High *Myb* levels were especially found in acute myeloid leukemia (AML).²⁻⁴ *Myb* was identified initially as a retroviral oncogene (*v-Myb*) of avian myeloblastosis virus and E26.^{5,6} These retroviruses are able to transform immature hematopoietic cells in vitro and induce AMLs in chickens⁷ and mice.⁸ In leukemia patients, *MYB* is highly expressed, and in a subset of patients, this is a consequence of translocations, genomic duplications, or somatic mutations that involve the *MYB* gene itself.⁹⁻¹² Furthermore, compelling evidence is accumulating that MYB also acts as a dependency factor for the maintenance of most myeloid, T-, and B-cell leukemias.¹³⁻¹⁵ Overexpression of viral MYB, a truncated form of MYB that lacks its negative regulatory domain, results in the spontaneous formation of T-cell lymphomas in mice.¹⁶ However, the in vivo roles of cellular MYB in tumor initiation remain largely unexplored. Here, we show, for the first time, that hematopoietic-specific overexpression of *Myb* is sufficient to drive B-cell neoplasms and myeloid malignancies in mice.

To evaluate whether elevated *MYB* expression is sufficient to transform cells in vivo, we developed a conditional *Myb* overexpression (*R26-Myb*) mouse model (Figure 1A; supplemental Figure 1A,B) using an optimized pipeline for targeting the *Rosa26* (*R26*) locus,¹⁷ which previously allowed us to model AML,¹⁷ mantle cell lymphoma,¹⁸ and immature T-cell leukemia¹⁹ in mice. Cre-mediated removal of the floxed stop cassette in mouse embryonic stem cells resulted in a 10-fold increase of *Myb* transcripts and a threefold upregulation of MYB protein (supplemental Figure 1C,D). *R26-Myb* mice were crossed with *Vav-iCre* mice²⁰ to enable *R26*-driven overexpression of *Myb* and a *Firefly luciferase*-reporter in the entire hematopoietic system (supplemental Figure 1E). Homozygous *R26-Myb* mice have a 10- to 15-fold increase in *Myb* RNA levels in the thymus and bone marrow (BM) (supplemental Figure 1F,G). Of note, we were not able to show increased MYB protein level of 10-week-old thymocytes (data not shown), probably because T-cell progenitors already express high endogenous MYB levels. We monitored an aging cohort of *R26-Myb^{tg/tg}; Vav-iCre^{tg/+}* (hereafter named *Myb^{Vav}*, n = 21 with 9 males and 12 females) mice (Figure 1A) and found that 7 out of 21 (33%) animals spontaneously developed hematological malignancies (Figure 1B). Detailed necropsy was performed on 4 animals. *Myb^{Vav}* mice had mild anemia and showed increased white blood cell and lymphocyte counts in peripheral blood (Figure 1C). In addition, 3 of them displayed splenomegaly (Figure 1D). Detailed flow cytometric analysis revealed that *Myb* overexpression resulted in the spontaneous development of both B-cell neoplasms and myeloid malignancies (Figure 1E,F). A selection of 1 *Myb^{Vav}* tumor per mouse is represented in Figure 1E, while an overview of the immunophenotype of all *Myb^{Vav}* tumors per mouse is shown in Figure 1F. A comparison of these *Myb^{Vav}* tumors with their Cre-negative littermate controls can be found in supplemental Figure 2. Although cumulative genetic evidence suggests a role for *Myb* in T-cell

Submitted 16 August 2021; accepted 29 December 2021; prepublished online on *Blood Advances* First Edition 12 January 2022; final version published online 16 May 2022. DOI 10.1182/bloodadvances.2021005955.

*T.P., A.A., S.G., and P.V.V. contributed equally to this work.

Requests for data sharing may be submitted to Pieter Van Vlierberghé (Pieter.vanvlierberghé@ugent.be).

The full-text version of this article contains a data supplement.

© 2022 by The American Society of Hematology. Licensed under Creative Commons Attribution-NonCommercial-NoDerivatives 4.0 International (CC BY-NC-ND 4.0), permitting only noncommercial, nonderivative use with attribution. All other rights reserved.

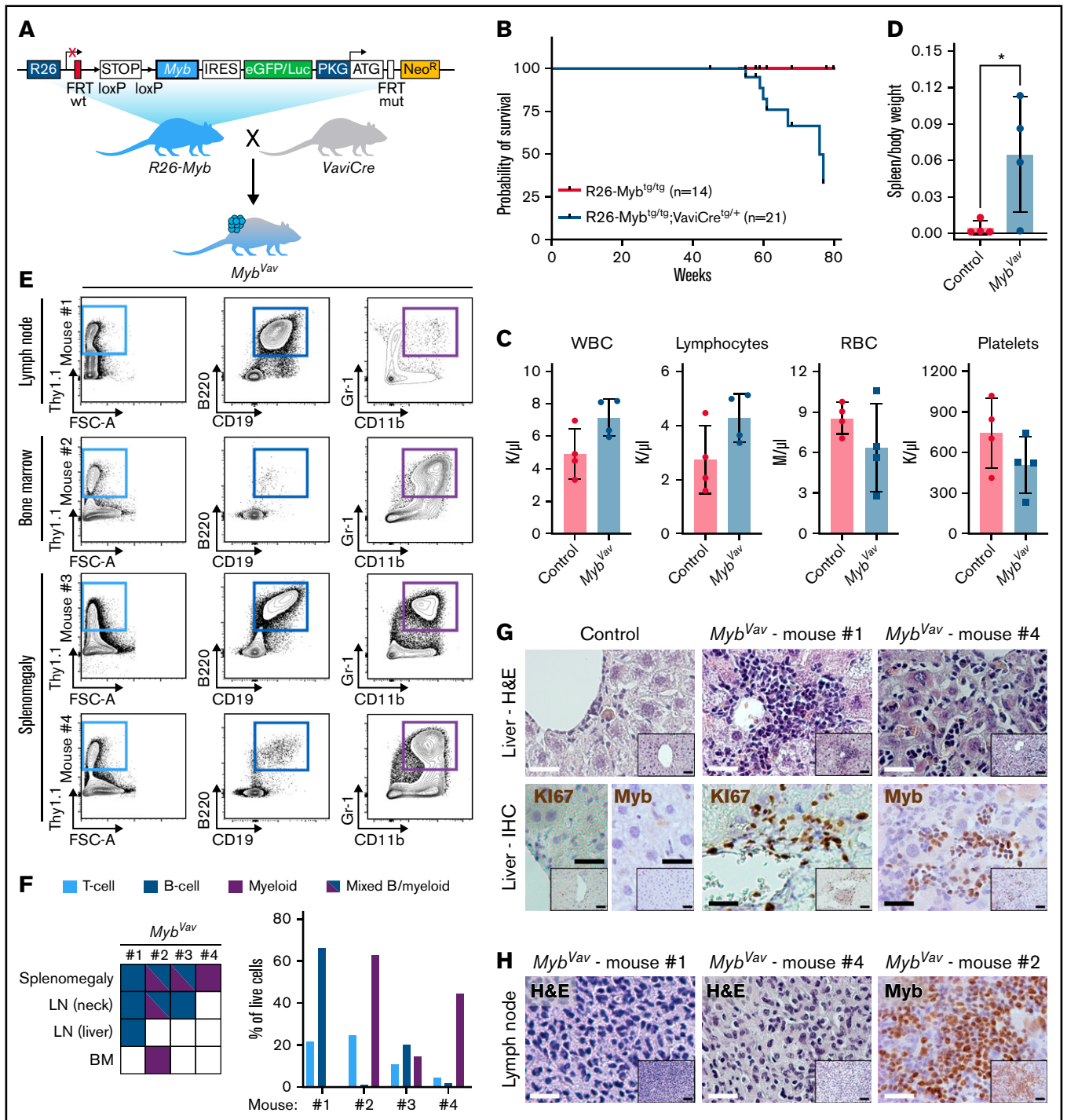


Figure 1. Myb overexpression enables the formation of B-cell and myeloid neoplasms in vivo. (A) Schematic representation of *R26-Myb* mice that allow Cre-dependent conditional expression of a bicistronic transgene transcript, encoding for Myb and the eGFP/Luciferase reporter, from the *Rosa26* promoter. Breeding scheme to obtain *R26-Myb^{tg/tg};VaviCre^{tg/+}* (*Myb^{Vav}*) mice with hematopoietic-specific overexpression of Myb. R26, *Rosa26*; IRES, independent ribosomal entry site; eGFP, enhanced green fluorescent protein; PKG, phosphoglycerate kinase 1; Neo^R, neomycin resistance gene. (B) Kaplan Meier survival curve of Cre-negative control (*R26-Myb^{tg/tg}*) vs *Myb^{Vav}* mice. A log-rank Mantel-Cox test showed that survival of *Myb^{Vav}* mice was significantly lower. **P* = .0302. (C) Peripheral blood values of *Myb^{Vav}* mice and nonrecombined controls. WBC, white blood cells; RBC, red blood cells. An unpaired *t*-test indicated that there was no significant difference between tumor-carrying *Myb^{Vav}* mice and nonrecombined controls. (D) Graph depicting the spleen-to-body weight ratio of *Myb^{Vav}* mice that developed neoplasm and age-matched Cre-negative littermate control mice. **P* = .0450. (E) Flow cytometry analysis of 4 *Myb^{Vav}* tumors. Single live cells were analyzed for the T-cell marker Thy1.1 (CD90), B-cell markers B220 and CD19, and myeloid markers Gr-1 and Cd11b. FSC-A, forward scatter area. (F) Left: heatmap summarizing flow data of tumor samples, including BM, LN, and spleen, from 4 *Myb^{Vav}* mice. Right: Graph depicting the percentage of T cells, B cells, or myeloid cells from panel E, which were pre-gated for single live cells. (G,H) Hematoxylin and eosin (H&E) staining or representative immunohistochemistry (IHC) for the proliferation marker KI67 or MYB on paraffin sections of *Myb^{Vav}* liver (G) and LN (H) tumors and of an age-matched Cre-negative littermate control. Scale bar: 25 μ m. Scale bar inset: 50 μ m.

leukemia,⁹⁻¹¹ no spontaneous T-cell malignancies were observed in *Myb*^{Vav} mice. One explanation for this might be that *Myb* is already highly expressed in T-cell progenitors and that the additional R26-driven *Myb* does not have a major impact on the already high *Myb* levels in this lineage. One *Myb*-driven malignancy displayed increased percentages of conventional CD19⁺B220⁺ B cells in the liver and spleen compared with the corresponding organs of nondiseased Cre⁻ littermate controls (supplemental Figure 2A). B-cell populations in this *Myb*^{Vav} tumor (mouse #1) reached 44% and 58% in the spleen and lymph node (LN), respectively, while T-cell and myeloid populations were only underrepresented (supplemental Figure 2B,C). Two *Myb*^{Vav} mice (mouse #2 and #4) had tumors that displayed dominant myeloid cell fractions in BM (62%) and splenomegaly (44%), respectively (Figure 1E,F). Here, the percentage of myeloid cells in the spleen and BM of mouse #2 was higher compared with nondiseased Cre⁻ littermate control samples (supplemental Figure 2D). Remarkably, the lymphoma and spleen samples of *Myb*^{Vav} mouse #2 and the spleen sample of *Myb*^{Vav} mouse #3 presented with mixed immunophenotype malignancies, which were composed of both B cells and myeloid cells (Figure 1E,F). We wondered if these mixed *Myb*^{Vav} malignancies were of ambiguous lineage, featuring both myeloid and B-cell markers on the same cell, or biphenotypic containing a mixture of both B- and malignant myeloid cells. By using flow cytometry, we confirmed that mixed *Myb*^{Vav} malignancies were biphenotypic, containing both B- and malignant myeloid cells (supplemental Figure 2E). The lymphoid and myeloid features of the *Myb*^{Vav} tumors were validated via histology, including liver infiltration of Ki67- and MYB-positive tumor cells via the portal vein (Figure 1G; mouse #1 and right panel) or liver sinusoids (Figure 1G; mouse #4), which are typically observed in lymphoid and myeloid leukemias. All examined liver (n = 2) and LN (n = 3) infiltrations in *Myb*^{Vav} mice were composed of MYB-positive cells (Figure 1G,H).

Next, we investigated whether these *Myb*-driven hematological malignancies could be transplanted into secondary recipients and could grow out as full-blown myeloid or B-cell malignancies (Figure 2A). The transgenic animals and derived malignant cells express a bicistronic transgene transcript that encodes both *Myb* as well as the *Firefly luciferase*-reporter (Figure 1A), which enables us to trace neoplastic cells upon transplantations in secondary hosts using in vivo bioluminescence imaging. In a first transplantation experiment, we transplanted 4 primary *Myb*^{Vav} tumors from 3 mice (#1, #2, and #4), and engraftment in immunodeficient nonobese diabetic/severely compromised immunodeficiency γ (NSG) mice was observed using myeloid tumor material obtained from BM (*Myb*^{Vav} mouse #2) (Figure 2B). In line with the bioluminescence data, a secondary neoplasm was identified in the BM of this NSG 21 weeks posttransplantation (Figure 2B), and the myeloid origin of the luciferase-positive transplanted material was confirmed by flow cytometry (Figure 2C-E; transplant #2). We monitored a second series of *Myb*^{Vav} transplants (6 primary tumors from 4 *Myb*^{Vav} mice) for 40 weeks, and although engraftment of a low number of luciferase-positive myeloid or B cells could be observed (Figure 2C-E), no secondary malignancies were formed within 40 weeks. Since no B-cell tumors formed secondary neoplasms upon transplantation, they should be called B-cell proliferative disease rather than B-cell malignancies. This also suggests that additional oncogenic hits and/or an immunocompetent microenvironment may be required in order to promote full-blown malignant transformation of *Myb*^{Vav} tumors.

In conclusion, we modeled aberrant MYB overexpression, which is observed in many types of cancer, including breast and colon cancer, and hematological malignancies, using a newly established conditional *Myb* overexpression mouse model. We show that hematopoietic-specific overexpression of *Myb* is sufficient to induce B-cell neoplasms and myeloid malignancies in vivo, providing evidence for its function as an oncogene in the initiation of myeloid leukemia. Our data confirm the longstanding relationship between elevated *Myb* expression in myeloid leukemias¹⁻⁴ and its high transformation potential in chicken and mice.^{7,8,16,21,22} In contrast, the newly identified role for *Myb* in the initiation of B-cell lymphoproliferative disease is rather unexpected as up to now, *MYB* was only associated with maintenance of B-cell leukemias.¹⁵ This conditional *R26-Myb* mouse model might also be of value to elucidate the role of MYB during the initiation of, for instance, breast or colon cancer.

Besides its role in tumor initiation, MYB also plays an important role in the maintenance of both AML and acute lymphoblastic leukemias,^{13,15} a notion that was confirmed in large scale functional screenings performed by the Broad Institute (data from the Cancer Dependency Map; <https://depmap.org/portal/>) (Figure 2F) using CRISPR/CAS9 knockouts and short hairpin RNA-mediated knock-down on 802 human cancer cell lines. The 20 AML and 10 ALL cell lines in this data set were significantly more dependent on *MYB* expression compared with nonleukemic cell lines (n = 772) (Figure 2F). Based on this observation, we wondered whether the murine *Myb*-driven B-cell neoplasms and myeloid malignancies relied on the continued transcriptional activity of *Myb* for their survival. MYB is a transcription factor and has a tripartite structure with an N-terminal DNA-binding domain, a central transactivation domain (TAD), and a C-terminal negative regulatory domain.^{1,23} The TAD of MYB allows the recruitment of its coactivators, such as CBP or its paralogue p300, through their KIX domain. It was shown that the interaction between MYB and CBP/p300 is required for leukemogenesis. Especially, MYB residue E308 is essential for this interaction, as was elegantly shown in the *Booreana* mouse strain, which has a naturally occurring *Myb* E308G mutation and is resistant to AML1-ETO- or MLL-AF9-induced leukemogenesis.²⁴ Therefore, blocking the interaction between MYB and its transcriptional coactivators CBP/p300 is an attractive therapeutic strategy to treat AML. Indeed, human AML cells were effectively killed when the MYB:CBP/P300 binding was blocked with MYBMIM, a cell-penetrant peptidomimetic inhibitor that contains MYB residues 293-310.²⁵ In contrast, human AML cell viability was unaffected when treated with an inactive version of MYBMIM, termed TG3, in which 3 MYB residues, which are important for the interaction with CBP/p300 (including E308), were replaced with glycines.²⁵ Here, we confirmed that *Myb*-driven murine myeloid malignancies were also sensitive to MYBMIM (Figure 2G), using concentrations that were comparable to those that were used to effectively induce apoptosis and differentiation of human AMLs.²⁵ At these concentrations, TG3 treatment had no significant effect on the viability of *Myb*-driven myeloid malignancies (Figure 2G). Finally, we also treated murine B-cell or mixed *Myb*^{Vav} malignancies with either MYBMIM or TG3 and found that these malignancies were also selectively sensitive to MYBMIM treatment (Figure 2G). It remains to be determined if this reduction in cell viability is due to reduced cell proliferation or increased apoptosis. Our results confirm that MYB is not only sufficient to initiate myeloid malignancies but that MYB is also required for tumor maintenance.

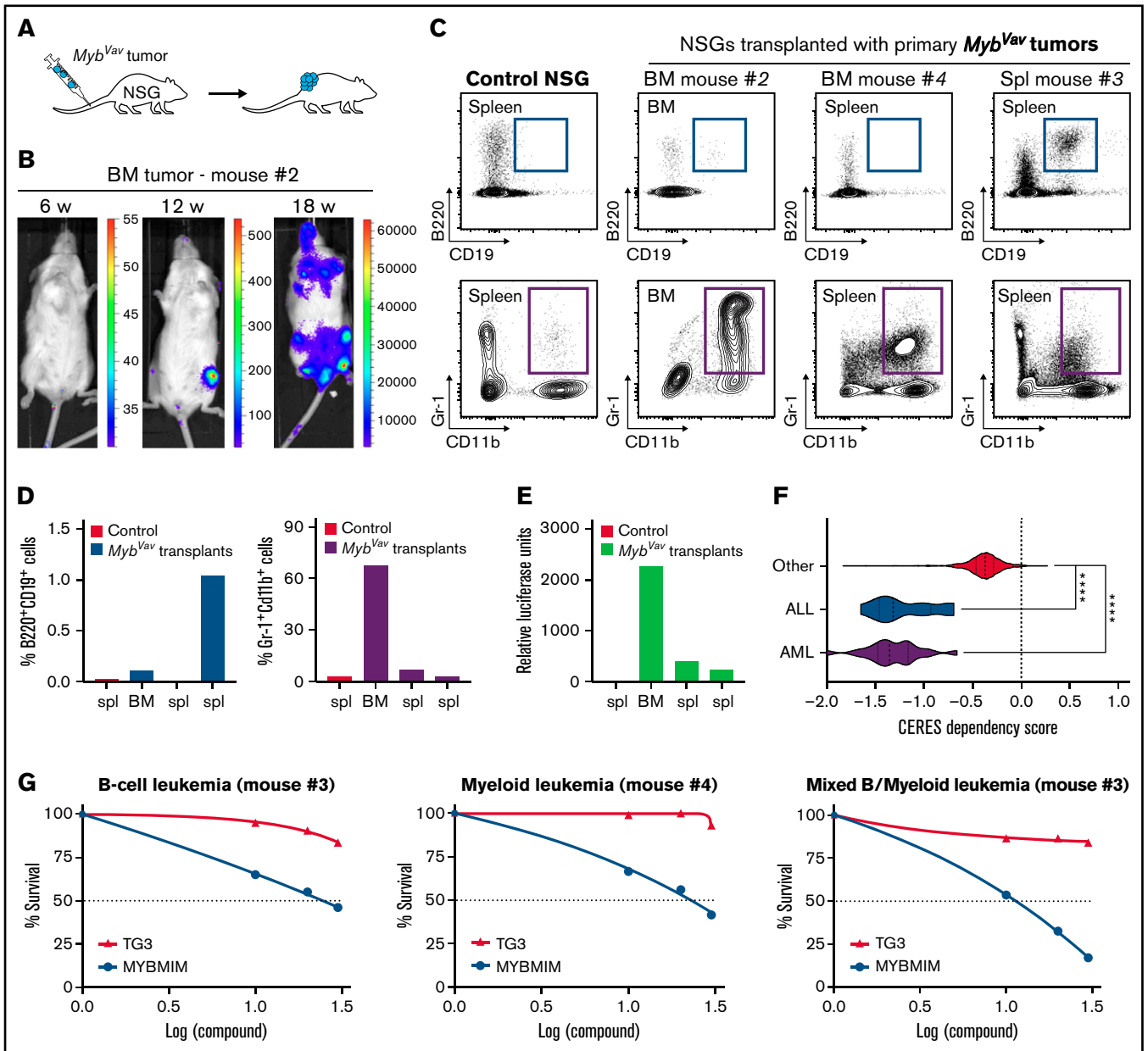


Figure 2. Transplantation and therapeutic targeting of the transcriptional activity of Myb. (A) Scheme of primary transplantation of *Myb^{Vav}* tumor cells into immunocompromised nonobese diabetic/severely compromised immunodeficiency γ (NSG) mice. (B) Bioluminescence of a primary BM tumor sample from *Myb^{Vav}* mouse #2 that was transplanted in an NSG mouse. Bioluminescence was measured over time. (C) Flow cytometry analysis of myeloid ($Gr-1^+ Cd11b^+$) and B cells ($B220^+ CD19^+$) of a control NSG and NSGs that were transplanted primary *Myb^{Vav}* tumor cells. (D) Graphs showing the percentage of B cells or myeloid cells which were pre-gated for single live cells. (E) Luciferase assay on *Myb^{Vav}* transplants. (F) Violin plots showing CERES cell dependency scores for MYB from AML ($n = 20$), ALL ($n = 10$), and 772 other cancer cell lines which were taken from DepMap (<https://depmap.org/portal/>). CERES is a computational method that estimates gene dependency based on data from CRISPR-Cas9 screens. A CERES score of 0 indicates that MYB is not essential, while a lower score indicates a higher likelihood that MYB is essential in a given cell line. MYB, AML, and ALL cell lines had a significantly lower CERES score than other cell lines. **** $P < .0001$. (G) Graphs depicting the survival of myeloid, B-cell, and mixed B/myeloid hematopoietic malignancies, which were treated for 48 hours with increasing concentrations of either MYBMIM or TG3.

In conclusion, and in line with the notion that *MYB* is highly expressed and required in both B-cell and myeloid malignancies^{2,13,15} and has in vitro transformation potential,^{21,22} we show that *Myb* drives spontaneous B-cell neoplasms and myeloid malignancies in mice.

Acknowledgments: The authors thank Jinke D'Hont and Frédérique Van Rockeghem for technical assistance.

This work was supported by the Baillet Latour Foundation, the Ghent University Research Fund (BOF-UGent), and the Research Foundation Flanders (FWO).

Contribution: T.P., A.A., S.T., K.L., and T.H. performed research; G.B. and A.K. provided research tools; and T.P., S.G., and P.V.V. designed research and wrote the paper.

Conflict-of-interest disclosure: A.K. is a consultant for Novartis and Rgenta. All other authors declare no competing financial interests.

ORCID profiles: A.A., 0000-0001-5282-7278; S.T., 0000-0003-4256-9775; S.G., 0000-0002-5693-8570; P.V.V., 0000-0001-9063-7205.

Correspondence: Pieter Van Vlierberghe, Department of Biomolecular Medicine, Ghent University, Corneel Heymanslaan 10, 9000 Ghent, Belgium; e-mail: pieter.vanvlierberghe@ugent.be.

References

1. Ramsay RG, Gonda TJ. MYB function in normal and cancer cells. *Nat Rev Cancer*. 2008;8(7):523-534.
2. Pattabiraman DR, Gonda TJ. Role and potential for therapeutic targeting of MYB in leukemia. *Leukemia*. 2013;27(2):269-277.
3. Ferrari S, Torelli U, Selleri L, et al. Study of the levels of expression of two oncogenes, c-myc and c-myb, in acute and chronic leukemias of both lymphoid and myeloid lineage. *Leuk Res*. 1985;9(7):833-842.
4. Rosson D, Tereba A. Transcription of hematopoietic-associated oncogenes in childhood leukemia. *Cancer Res*. 1983;43(8):3912-3918.
5. Weinstein Y, Ihle JN, Lavu S, Reddy EP. Truncation of the c-myb gene by a retroviral integration in an interleukin 3-dependent myeloid leukemia cell line. *Proc Natl Acad Sci USA*. 1986;83(14):5010-5014.
6. Leprince D, Gegonne A, Coll J, et al. A putative second cell-derived oncogene of the avian leukaemia retrovirus E26. *Nature*. 1983;306(5941):395-397.
7. Beug H, von Kirchbach A, Döderlein G, Conscience JF, Graf T. Chicken hematopoietic cells transformed by seven strains of defective avian leukemia viruses display three distinct phenotypes of differentiation. *Cell*. 1979;18(2):375-390.
8. Shen-Ong GL, Potter M, Mushinski JF, Lavu S, Reddy EP. Activation of the c-myb locus by viral insertional mutagenesis in plasmacytoid lymphosarcomas. *Science*. 1984;226(4678):1077-1080.
9. Clappier E, Cucuini W, Kalota A, et al. The C-MYB locus is involved in chromosomal translocation and genomic duplications in human T-cell acute leukemia (T-ALL), the translocation defining a new T-ALL subtype in very young children. *Blood*. 2007;110(4):1251-1261.
10. Lahortiga I, De Keersmaecker K, Van Vlierberghe P, et al. Duplication of the MYB oncogene in T cell acute lymphoblastic leukemia. *Nat Genet*. 2007;39(5):593-595.
11. Liu Y, Easton J, Shao Y, et al. The genomic landscape of pediatric and young adult T-lineage acute lymphoblastic leukemia. *Nat Genet*. 2017;49(8):1211-1218.
12. Belloni E, Shing D, Tapinassi C, et al. In vivo expression of an aberrant MYB-GATA1 fusion induces leukemia in the presence of GATA1 reduced levels [published correction appears in *Leukemia*. 2011;25(12):1922]. *Leukemia*. 2011;25(4):733-736.
13. Zuber J, Rappaport AR, Luo W, et al. An integrated approach to dissecting oncogene addiction implicates a Myb-coordinated self-renewal program as essential for leukemia maintenance [published correction appears in *Genes Dev*. 2011;25(18):1997]. *Genes Dev*. 2011;25(15):1628-1640.
14. Sanghvi VR, Mavrakis KJ, Van der Meulen J, et al. Characterization of a set of tumor suppressor microRNAs in T cell acute lymphoblastic leukemia. *Sci Signal*. 2014;7(352):ra1111.
15. De Dominicis M, Porazzi P, Soliera AR, et al. Targeting CDK6 and BCL2 exploits the "MYB addiction" of Ph(+) acute lymphoblastic leukemia. *Cancer Res*. 2018;78(4):1097-1109.
16. Badiani PA, Kioussis D, Swirsky DM, Lampert IA, Weston K. T-cell lymphomas in v-Myb transgenic mice. *Oncogene*. 1996;13(10):2205-2212.
17. Pieters T, T'Sas S, Demoen L, et al. Novel strategy for rapid functional in vivo validation of oncogenic drivers in haematological malignancies. *Sci Rep*. 2019;9(1):10577.
18. Pieters T, T'Sas S, Vanhee S, et al. Cyclin D2 overexpression drives B1a-derived MCL-like lymphoma in mice. *J Exp Med*. 2021;218(10):e20202280.
19. Goossens S, Radaelli E, Blanchet O, et al. ZEB2 drives immature T-cell lymphoblastic leukaemia development via enhanced tumour-initiating potential and IL-7 receptor signalling. *Nat Commun*. 2015;6(1):5794.
20. de Boer J, Williams A, Skavdis G, et al. Transgenic mice with hematopoietic and lymphoid specific expression of Cre. *Eur J Immunol*. 2003;33(2):314-325.
21. Radke K, Beug H, Kornfeld S, Graf T. Transformation of both erythroid and myeloid cells by E26, an avian leukemia virus that contains the myb gene. *Cell*. 1982;31(3 Pt 2):643-653.
22. Moscovici C, Samarut J, Gazzolo L, Moscovici MG. Myeloid and erythroid neoplastic responses to avian defective leukemia viruses in chickens and in quail. *Virology*. 1981;113(2):765-768.
23. Oh IH, Reddy EP. The myb gene family in cell growth, differentiation and apoptosis. *Oncogene*. 1999;18(19):3017-3033.
24. Pattabiraman DR, McGirr C, Shakhbazov K, et al. Interaction of c-Myb with p300 is required for the induction of acute myeloid leukemia (AML) by human AML oncogenes. *Blood*. 2014;123(17):2682-2690.
25. Ramaswamy K, Forbes L, Minuesa G, et al. Peptidomimetic blockade of MYB in acute myeloid leukemia. *Nat Commun*. 2018;9(1):110.